International Journal of Heat and Mass Transfer 52 (2009) 5005–5012

Contents lists available at ScienceDirect

International Journal of Heat and Mass Transfer

journal homepage: www.elsevier.com/locate/ijhmt

Numerical study of a nuclear fuel element dissipating fission heat into its surrounding fluid medium

M.K. Ramis, G. Jilani *

Department of Mechanical Engineering, National Institute of Technology Calicut, Kerala 673 601, India

ARTICLE INFO

Article history:
Received 11 April 2008
Received in revised form 26 March 2009
Accepted 3 April 2009
Available online 25 June 2009

Keywords:
Conjugate heat transfer
Nuclear fuel element
Finite difference schemes
Conduction–convection parameter
Volumetric energy generation

ABSTRACT

The objective of the present work is twofold – the first to establish the criterion for the boundary layer solution to be accurate enough in the study of conjugate heat transfer problem associated with a rectangular nuclear fuel element washed by upward moving coolant and the second to predict the critical thermal performance characteristics of the fuel element with uniform volumetric energy generation. Accordingly, employing stream function–vorticity formulation, equations governing the steady, two-dimensional flow and thermal fields in the coolant are solved simultaneously with the steady, two-dimensional heat conduction equation for the fuel element using second-order accurate finite difference schemes. Keeping the Prandtl number constant at 0.005 for liquid sodium as coolant, numerical results are presented for wide range of aspect ratio, conduction–convection parameter, energy generation parameter and Reynolds number. It is found that for all value of aspect ratio greater than 15, numerical prediction using the boundary layer approximation based model is quite accurate enough. It is also concluded that other parameters being kept constant, the increase in the maximum fuel element temperature due to increase in aspect ratio beyond 15 is negligible. Further, it is found that a relatively higher value of conduction–convection parameter reduces the coolant pumping power requirement to a large extent.

1. Introduction

Ever since, the world's first nuclear reactor was commissioned at the University of Chicago, USA, a number of nuclear reactors are being built worldwide mainly to meet the ever-increasing demand of energy. Nuclear reactors are highly complex installations and hence utmost care is needed while designing them. The energy released due to fission within a fuel element of a nuclear reactor ultimately gives rise to an increase in its temperature. Therefore, the energy generated within a fuel element has to be dissipated fast enough in such a manner that its maximum temperature remains well within its allowable limit and the power developing capacity of the reactor is maximum. Keeping these two factors into consideration, the fuel elements in a reactor are cooled by an appropriate coolant flowing past over them. In the literature, the resulting heat transfer problem is referred to as 'conjugate heat transfer' problem in which the problem of heat conduction within the solid is solved simultaneously with that of forced convection over its lateral surface by satisfying the conditions of continuity of temperature and heat flux at the solid–fluid interface. There are many other important applications in which conjugate heat transfer occurs. A detail account of such examples can be found in the literature [1,2].

Owing to its occurrence in many engineering and practical applications, conjugate heat transfer problems associated with plate that is washed by a hot or a cold fluid have been the subjects of many investigations until recent past. Perelman [3] was probably the first to study analytically the conjugate heat transfer problem associated with the forced convection flow over a thin plate with a volumetric heat source. Subsequently, quite a good number of investigators have analytically/numerically studied the conjugate heat transfer problem associated with forced convection boundary layer type flow over a flat plate of finite thickness with its lower surface maintained at a constant temperature [4–10]. Several numerical studies on conjugate heat transfer problems arising out of a plate fin washed by forced convection boundary layer type of flow are reported in the literature [11–15]. Vynnycky et al. [16] studied analytically as well as numerically the conjugate heat transfer problem associated with forced convection flow over a conducting slab sited in an aligned uniform stream while its bottom surface maintained at uniform temperature. Conjugate heat transfer problem arising out of laminar plane wall jet flow over a heated slab was analyzed both analytically and numerically by Kanna and Das [17].

After Perelman [3], Karvinen [18] seems to be the second investigator who used an approximate method to study the conjugate

* Corresponding author. Tel.: +91 495 2286402; fax: +91 495 2287250.
E-mail address: jilani@nitc.ac.in (G. Jilani).

0017-9310/$ - see front matter © 2009 Elsevier Ltd. All rights reserved.
doi:10.1016/j.ijheatmasstransfer.2009.04.035

Nomenclature

Uppercase symbols given in the parentheses are the dimensionless counterparts of the dimensional equivalents written on the same line

A_r	aspect ratio of the fuel element
b (B)	width of the fluid domain
c_p	specific heat capacity of the coolant
C	geometric parameter
H	height of the fuel element
k	thermal conductivity
$\ell_o(L_o)$	length of the extended fluid domain at the trailing edge
N_{cc}	conduction–convection parameter
Pr	Prandtl number
q'''	volumetric energy generation
Q	energy generation parameter
Re_H	flow Reynolds number
T	temperature
T_o	maximum allowable temperature in fuel element
$u(U)$	velocity component in axial direction
U_∞	free stream velocity
$v(V)$	velocity component in transverse direction
$x(X)$	axial coordinate
y (Y)	transverse coordinate
W	half of the thickness of the fuel element

Greek symbols

θ	dimensionless temperature
ρ	density of the coolant
μ	dynamic viscosity of the coolant
Ψ	dimensionless stream function
Ω	dimensionless vorticity

Subscripts

f	fluid domain
s	solid domain
sf	solid–fluid interface
∞	free stream
max	maximum

heat transfer problem associated with forced convection flow over a thin heat generating plate. Jahangeer et al. [1] numerically analyzed the conjugate forced convection flow over a heat generating vertical plate. Deriving motivation from the work of Jahangeer et al. [1], Ramis et al. [2] carried out a numerical study on the conjugate heat transfer problem arising out of forced convection flow over a vertical plate with non-uniform heat generation.

An up-to-date review of the literature presented above reveals that with the exception of Jahangeer et al. [1], Ramis et al. [2], Perelman [3], and Karvinen [18], none of the studies pertains to the conjugate heat transfer analysis of a heat generating plate. While the analytical study of Perelman [3] deals with specific cases without any parametric study, the work of Karvinen [18] is based on the assumption of one-dimensional heat conduction in the plate. Although, the parametric studies of Jahangeer et al. [1] and Ramis et al. [2] considered two-dimensional heat conduction in the plate, numerical results presented by them are based on the solution of boundary layer equations. Deriving motivation from these studies, the present work aims at fulfilling two objectives – the first to establish the criterion for the boundary layer solution to be accurate enough in the study of conjugate heat transfer problem associated with a rectangular nuclear fuel element washed by upward moving coolant and the second to predict the critical thermal performance characteristics of the fuel element with uniform volumetric energy generation.

2. Mathematical formulation

Fig. 1 illustrates a physical model of a rectangular nuclear fuel element of height H, thickness $2W$ washed by upward flowing liquid sodium as coolant. The thermal conductivity of the material of the fuel element is denoted by k_s and density, dynamic viscosity, specific heat and thermal conductivity of the coolant are represented by the symbols ρ, μ, c_p, k_f, respectively. The coolant approaches the leading edge of the fuel element at uniform temperature T_∞ and uniform velocity U_∞. A Cartesian coordinate system is superimposed on the fuel element such that its origin coincides with the bottom-right corner of the fuel element and its x-coordinate is directed upward along the solid–fluid interface while the y-coordinate is marked towards the right direction as shown in the figure. Under steady state operating conditions of the nuclear reactor, while the leading edge of the fuel element is assumed to be in perfect thermal contact with the oncoming stream of coolant, thereby, maintained at temperature T_∞, the heat dissipation from its trailing edge is considered negligibly small. The volumetric energy generation q''' due to fission reaction is assumed to be uniform everywhere in the fuel element. This fission energy generated in the fuel element is first conducted within it and finally dissipated from its lateral surface by forced convection to the upward moving streams of coolant so as to keep the maximum temperature T_0 in the fuel element well within its allowable limit. In order to impose physically meaningful supplementary conditions, the outflow boundary of the flow and thermal fields

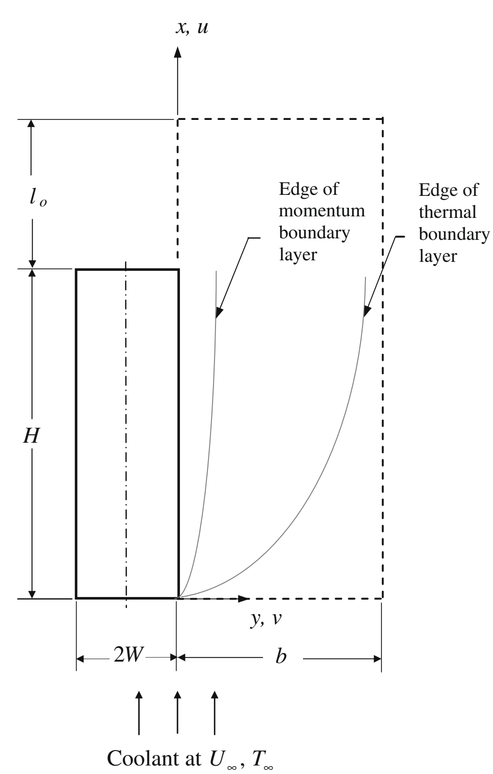

Fig. 1. Physical model.

are located at a distance l_o downstream of the trailing edge of the fuel element as shown in Fig. 1. Also, the right boundary of the flow and thermal fields in the fluid domain is located at a distance b from the solid–fluid interface, which is not known *a priori* and has to be ascertained by numerical experimentation.

In order to represent this physical model of the problem stated above into a mathematical model, the following additional approximations and assumptions are introduced:

(i) The material of the fuel element is homogeneous and isotropic.
(ii) The thermal conductivity of the fuel element is independent of temperature.
(iii) The temperature gradient normal to the x–y plane is negligibly small.
(iv) The flow is steady, laminar, incompressible and two-dimensional.
(v) The coolant is Newtonian and viscous.
(vi) The thermo-physical properties of the coolant are constant.

Introducing the approximations and assumptions listed above and employing stream function–vorticity formulation, the dimensionless equations governing the flow and thermal fields in the upward moving stream of coolant can be obtained as:

Stream function:

$$\frac{\partial^2 \Psi}{\partial X^2} + \frac{\partial^2 \Psi}{\partial Y_f^2} = -\Omega \tag{1}$$

where the dimensionless stream function, Ψ and dimensionless vorticity, Ω appearing in Eq. (1) are defined as:

$$U = \frac{\partial \Psi}{\partial Y_f}, \quad V = -\frac{\partial \Psi}{\partial X}, \quad \text{and } \Omega = \frac{\partial V}{\partial X} - \frac{\partial U}{\partial Y_f} \tag{2}$$

Vorticity transport:

$$U\frac{\partial \Omega}{\partial X} + V\frac{\partial \Omega}{\partial Y_f} = \frac{1}{Re_H}\left(\frac{\partial^2 \Omega}{\partial X^2} + \frac{\partial^2 \Omega}{\partial Y_f^2}\right) \tag{3}$$

Energy:

$$U\frac{\partial \theta_f}{\partial X} + V\frac{\partial \theta_f}{\partial Y_f} = \frac{1}{Re_H \Pr}\left(\frac{\partial^2 \theta_f}{\partial X^2} + \frac{\partial^2 \theta_f}{\partial Y_f^2}\right) \tag{4}$$

The most appropriate boundary conditions to be specified can be written in dimensionless form as:

$$\begin{aligned}
&Y_f = 0; \quad 0 \le X \le 1, \quad \Psi = 0, \quad \Omega = -\frac{\partial^2 \Psi}{\partial Y_f^2}, \quad \frac{\partial \theta_f}{\partial Y_f} = \frac{1}{N_{cc}}\frac{\partial \theta_s}{\partial Y_s}\\
&Y_f = 0; \quad 1 < X \le (1 + L_o), \quad \Psi = 0, \quad \Omega = 0, \quad \frac{\partial \theta_f}{\partial Y_f} = 0\\
&Y_f = B; \quad 0 \le X \le (1 + L_o), \quad \Psi = \Psi_b, \quad \Omega = 0, \quad \frac{\partial \theta_f}{\partial Y_f} = 0\\
&X = 0; \quad 0 \le Y_f \le B, \quad \frac{\partial \Psi}{\partial X} = 0, \quad \Omega = 0, \quad \theta_f = 0\\
&X = (1 + L_o); \quad 0 \le Y_f \le B, \quad \frac{\partial \Psi}{\partial X} = 0, \quad \frac{\partial \Omega}{\partial X} = 0, \quad \frac{\partial \theta_f}{\partial X} = 0
\end{aligned} \tag{5}$$

The dimensionless form of equation governing the steady, two-dimensional heat conduction with uniform heat generation within the fuel element can be obtained as

$$\frac{\partial^2 \theta_s}{\partial X^2} + C\frac{\partial^2 \theta_s}{\partial Y_s^2} + CQ = 0 \tag{6}$$

where, C is a geometric parameter, which is defined as

$$C = 4A_r^2 \tag{7}$$

It is worth mentioning here that in addition to geometric symmetry, the flow and thermal fields in the solution domain are also symmetric about the vertical axis of the fuel element. Therefore, only half of the solution domain needs to be taken as the computational domain. Besides, these symmetries suggest that the transverse temperature gradient along the vertical axis of the fuel element is zero. The most appropriate supplementary conditions for the solution of Eq. (6) can be specified as

$$\begin{aligned}
&Y_s = -1; \quad 0 \le X \le 1, \quad \frac{\partial \theta_s}{\partial Y_s} = 0\\
&Y_s = 0; \quad 0 \le X \le 1, \quad \theta_s = \theta_f\\
&X = 0; \quad -1 \le Y_s \le 0, \quad \theta_s = 0\\
&X = 1; \quad -1 \le Y_s \le 0, \quad \frac{\partial \theta_s}{\partial X} = 0
\end{aligned} \tag{8}$$

The dimensionless variables and parameters appearing in Eqs. (1)–(8) is defined as

$$\begin{aligned}
&X = \frac{x}{H}, \quad Y_s = \frac{y}{W}, \quad Y_f = \frac{y}{H}, \quad U = \frac{u}{U_\infty},\\
&V = \frac{v}{U_\infty}, \quad \theta = \frac{T - T_\infty}{T_0 - T_\infty}, \quad A_r = \frac{H}{2W}, \quad B = \frac{b}{H},\\
&Q = \frac{q''' W^2}{k_s (T_0 - T_\infty)}, \quad N_{cc} = \frac{k_f}{k_s}\left[\frac{W}{H}\right], \quad L_0 = \frac{\ell_0}{H}, \quad Re_H = \frac{U_\infty H}{v}
\end{aligned} \tag{9}$$

In order to fulfill the first objective of this investigation, the numerical results obtained from the mathematical model as presented above are compared with those obtained from boundary layer approximation based mathematical model presented by Jahangeer et al. [1] and therefore, not reproduced here for the sake of brevity.

3. Numerical solution

Eqs. (1) and (3) for stream function and vorticity transport, respectively, are coupled and therefore, have to be solved simultaneously by employing an iterative solution procedure. Although, Eq. (4) for coolant temperature is uncoupled with these equations, it is also solved along with these equations as a part of numerical solution strategy being adopted. Accordingly, Eq. (1) along with its boundary conditions specified in Eq. (5) are discretized using second-order accurate finite difference schemes and the resulting system of finite difference equations are solved using 'Thomas Algorithm' and by employing 'Line-by-Line Gauss-Seidel' iterative solution procedure. On the other hand, pseudo-transient form of Eqs. (3) and (4) along with their boundary conditions given in Eq. (5) are discretized using Alternating Direction Implicit Scheme (ADI) and the resulting system of finite difference equations are solved using 'Thomas Algorithm'. Since, Eq. (6) for the fuel element temperature is coupled with Eq. (4) for coolant temperature; it has also to be solved along with the above mentioned equations by satisfying the continuity of temperature and heat flux at the solid–fluid interface. Thus, Eq. (6) along with boundary conditions specified in Eq. (8) is discretized using second-order accurate finite difference schemes and the resulting system of finite difference equations are solved using 'Thomas Algorithm' and by adopting 'Line-by-Line Gauss-Seidel' iterative solution procedure.

3.1. Validation of the computer code

A generalised computer code is developed exclusively for the present study. This computer code not only takes care of different kinds of boundary conditions but also generates numerical results associated with conjugate forced convection–conduction heat transfer from a rectangular plate with and without internal heat generation. Although the accuracy of the numerical results obtained from this code has been established at all stages of its development, the validity of the entire code is examined by comparing the temperature profiles at the solid–fluid interface obtained using the present code with those reported by Sparrow and Chyu [11] for a plate fin. At this point, it is to be made clear that the conduction–convection parameter N_{cc} as defined by Sparrow and Chyu [11] is $(4A_r^2 Re_H^{1/2})$ times more than that defined by us. Thus, in order to generate numerical results compatible with those presented by Sparrow and Chyu [11], our numerical value of N_{cc} (for aspect ratio $A_r = 5$ and Reynolds number $Re_H = 100$), turns out to be 10^3 times less than that of Sparrow and Chyu [11]. Fig. 2 illustrates the comparison of temperature profiles at the solid-fluid interface for three widely distinct values of N_{cc} as indicated on the figure. It can be seen that the numerical results obtained using the present code is in excellent agreement with those reported by Sparrow and Chyu [11]. Thus, the validity of the present computer code is established.

3.2. Grid independence test

In order to resolve the steep gradients present in the vicinity of the solid–fluid interface, the computational domain is superimposed with a finite difference mesh possessing variable grid pattern in the transverse direction while keeping the grid size uniform in the longitudinal direction. Moreover, keeping in view of the computational economy, an optimum grid pattern has to be chosen which in turn is ascertained by conducting a series of numerical experiments. During the course of these experiments, it is observed that the grid pattern strongly depends on flow Reynolds number Re_H. Thus, for each value of Re_H, a different set of numerical experiments is conducted in order to ascertain the optimum grid sizes to be used in the computation. Fig. 3(a and b) and Table 1 demonstrate one such grid independence test conducted for $Re_H = 2500$ by keeping $A_r = 15$, $N_{cc} = 0.4$, and $Q = 0.75$ as constant. Fig. 3(a) depicts the transverse temperature profiles at the axial location $X = 0.50$ in the fuel element for three different grid sizes, i.e., 21×81, 41×161, and 81×321, while Fig. 3(b) illustrates the transverse temperature profiles at the same axial location $X = 0.50$ in the fluid domain for three different grid sizes 46×106, 91×211, and 181×421. It can be noticed from these two figures that irrespective of the grid sizes used in both solid as well as fluid domains, the respective profiles superimpose each other. However, taking into the consideration of better resolution of the zero-Neumann boundary conditions in the computational domain, a grid size of 81×321 in the solid domain and 181×421 in the fluid domain is chosen for $Re_H = 2500$. Selection of these grid sizes is further justified by comparing the total energy generated within the fuel element with the total energy dissipated from its surfaces to the coolant as listed in Table 1 for the same three sets of grid sizes.

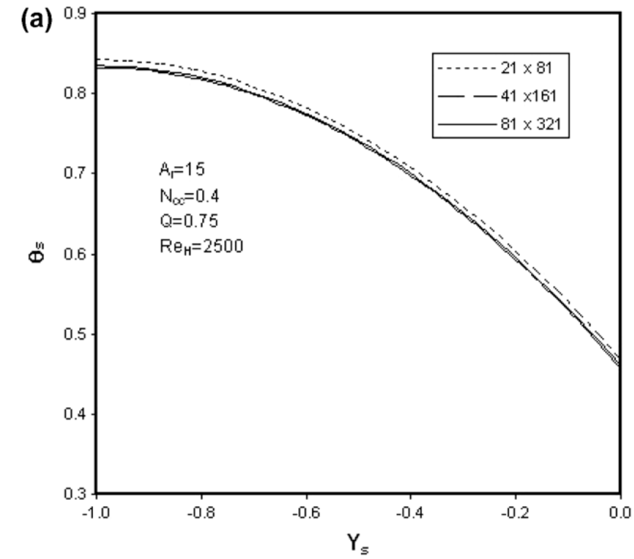

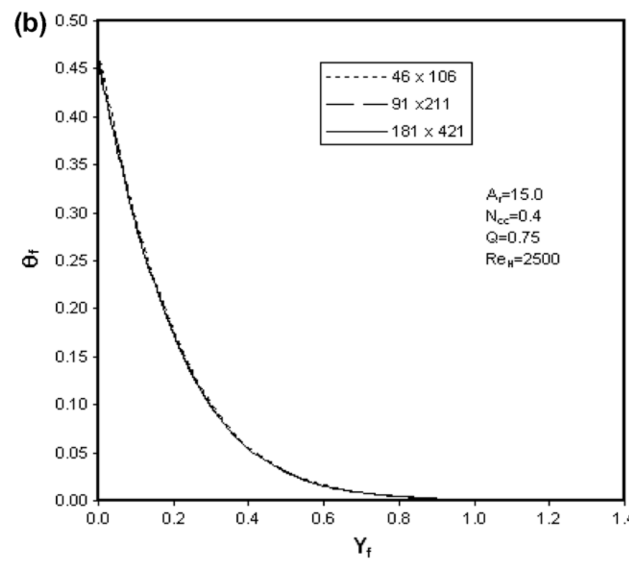

Fig. 3. (a) Transverse temperature profiles at $X = 0.5$ in the fuel element for three different grid sizes. (b) Transverse temperature profiles at $X = 0.5$ in the coolant for three different grid sizes.

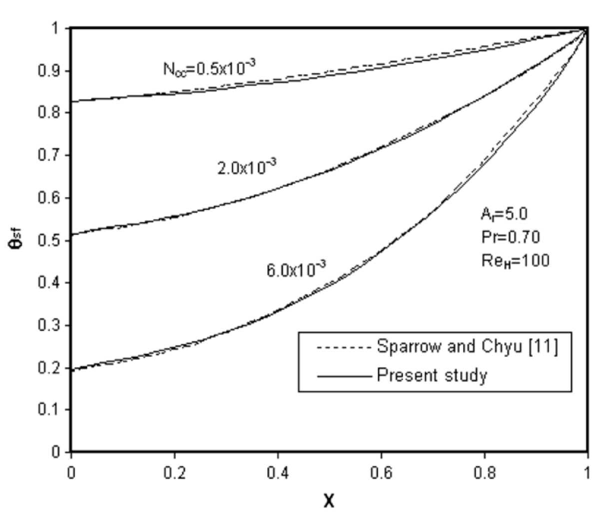

Fig. 2. Comparison of solid–fluid interface temperature profile with that of Sparrow and Chyu [11] for different conduction–convection parameter.

4. Results and discussions

The very first objective of the present investigation is to establish the criterion for boundary layer solution of the conjugate heat transfer problem associated with forced convection over a rectangular nuclear fuel element to be accurate enough. Accordingly, keeping Prandtl number constant at 0.005 for liquid sodium, the temperature profiles in the fuel element obtained from the numerical solution of the Full Navier–Stokes based mathematical model are compared with those obtained from the numerical solution of boundary layer approximation based mathematical model for different values of involved parameters. Keeping in view of the second objective, i.e., to predict the critical thermal performance characteristics of a rectangular fuel element, a critical analysis of

Table 1
Energy balance test conducted for three different grid sizes for $A_r = 15$, $N_{cc} = 0.4$, $Q = 0.75$ and $Re_H = 2500$.

Grid sizes		Heat Generation Parameter, Q (as input)	'Heat Generation Parameter Equivalent' at the two heat dissipating surfaces		
Solid	Fluid		Bottom surface, Q_b	Lateral surfaces, Q_l	$Q_b + Q_l$
21 × 81	46 × 106	0.75	0.017	0.724	0.741
41 × 161	91 × 211	0.75	0.018	0.726	0.744
81 × 321	181 × 421	0.75	0.019	0.726	0.745

the variation of maximum fuel element temperature θ_{max} with these involved parameters are presented and discussed in detail.

4.1. Axial temperature profiles

Fig. 4 depicts the effect of A_r on the axial temperature profiles along the centerline of the fuel element obtained using two different mathematical models. It is clearly evident from this figure that although the qualitative nature of the profiles corresponding to two different models is quite similar, the accuracy of the boundary layer approximation based model strongly depends on the value of A_r. It can be easily noticed that for a lower value of $A_r = 5$, the axial temperature profile obtained from boundary layer approximations based model is in substantial error except in the region close to the leading edge. In contrast, as depicted in this figure, a series of numerical experimentation reveals that for the value of $A_r \geqslant 15$, the axial temperature profile obtained using two different models more or less overlaps each other except in the region very close to the trailing edge. This disparity in the axial temperature profile near the trailing edge is due to artificial cooling of the trailing edge by the fluid in the extended computational domain employed in the solution of Full Navier–Stokes based model. The effect of N_{cc}, Q, and Re_H on the axial temperature profiles along the centerline of the fuel element obtained using two different mathematical models are illustrated in Figs. 5–7, respectively. Interestingly enough, it is very much evident from these figures that irrespective of the value of the parameters considered, the axial temperature profiles corresponding to two different models more or less overlap each other. Thus, one can easily conclude that irrespective of the values of other parameters, the numerical results obtained using boundary layer approximation based mathematical model is quite accurate enough for all values of $A_r \geqslant 15$.

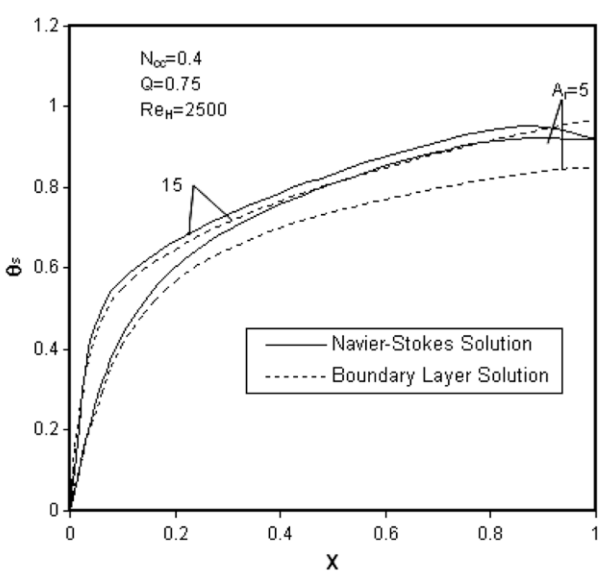

Fig. 4. Comparison of the effect of A_r on axial temperature profiles along the centerline of the fuel element between Navier–Stokes and boundary layer solutions.

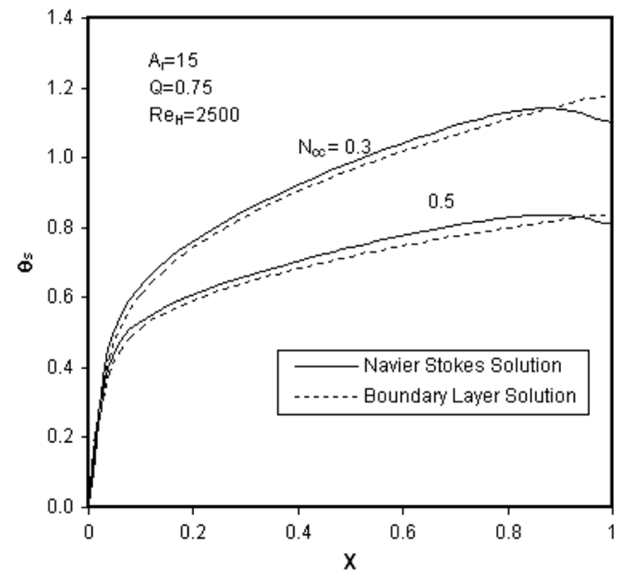

Fig. 5. Comparison of the effect of N_{cc} on axial temperature profiles along the centerline of the fuel element between Navier–Stokes and boundary layer solutions.

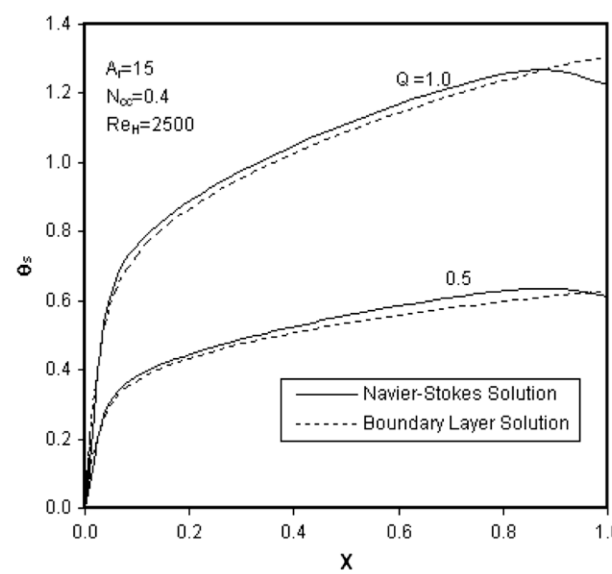

Fig. 6. Comparison of the effect of Q on axial temperature profiles along the centerline of the fuel element between Navier–Stokes and boundary layer solutions.

4.2. Critical parameters

Fig. 8 depicts the effect of A_r on the variation of θ_{max} with N_{cc} while $Q = 0.75$ and $Re_H = 2500$ are being kept constant. As expected, it can be easily seen that irrespective of the values of A_r, θ_{max} decreases monotonically with increase in N_{cc}. Further, it can be noted that increase in θ_{max} due to increase in A_r from its lower value 5 to

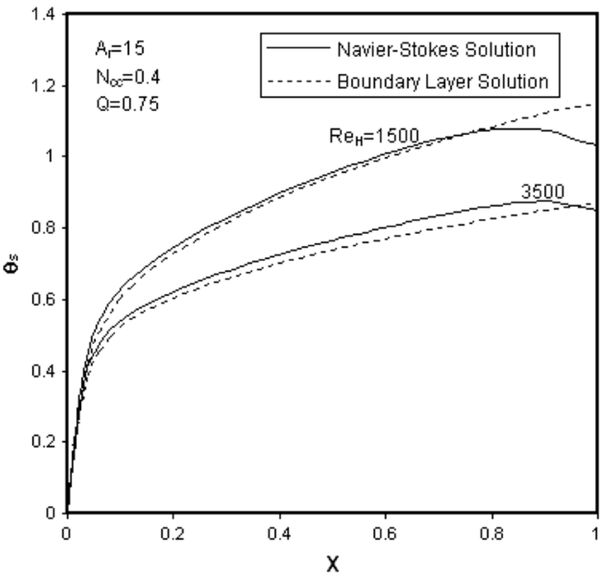

Fig. 7. Comparison of the effect of Re_H on axial temperature profiles along the centerline of the fuel element between Navier–Stokes and boundary layer solutions.

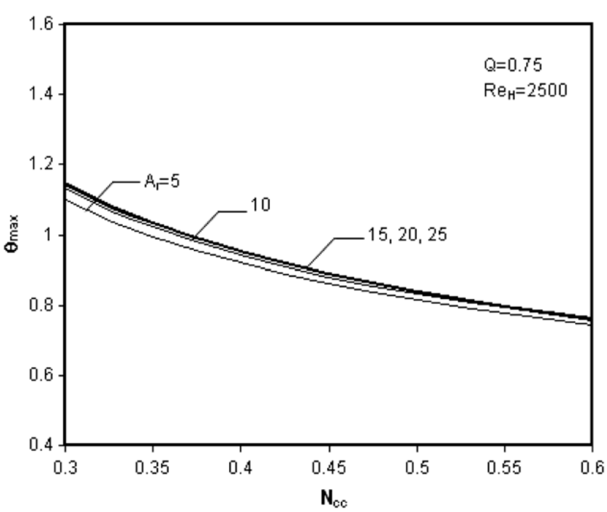

Fig. 8. The effect of A_r on the variation of θ_{max} with N_{cc}.

10 is quite marginal which even becomes insignificant for higher and higher values of N_{cc}.

Furthermore, it is important to note that for the entire range of N_{cc} values, an increase in A_r beyond 10, results in negligible increase in θ_{max}. Thus, it can be concluded from the preceding discussion that for a given set of constant parameters, there is an upper limiting value of A_r beyond which increase in θ_{max} is almost negligible. Also, it is extremely important to note that for a given value of A_r, there is a lower limiting value of N_{cc} below which the temperature in the fuel element crosses its allowable limit.

Fig. 9 illustrates the effect of Q on the variation of θ_{max} with N_{cc} while keeping $A_r = 15$ and $Re_H = 2500$ as constant. Similar to the trend seen in Fig. 8, it can be easily noted from this figure that irrespective of the value of Q, θ_{max} decreases monotonically with increase in N_{cc}. In addition, it is exclusively clear from this figure that rate of decrease in θ_{max} due to increase in N_{cc} is higher and higher for larger and larger values of Q. This is particularly true for all values of $N_{cc} < 0.40$. Further, it is quite important to note that for $Q = 0.50$ and the entire range of N_{cc}, the values of θ_{max} in the fuel

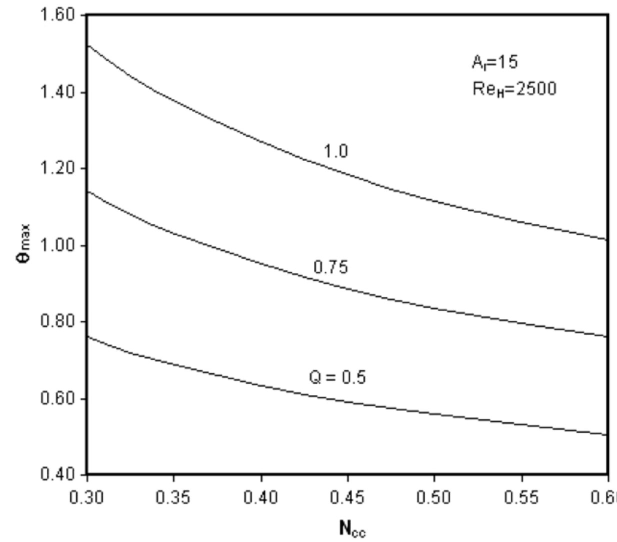

Fig. 9. The effect of Q on the variation of θ_{max} with N_{cc}.

element remains well within the allowable limit. In contrast to this, it is equally important to note that for $Q = 1.00$ and the whole range of N_{cc}, the corresponding values of θ_{max} crosses its permissible limit. Interestingly enough, it is very much evident from this figure that for any intermediate value of Q, there is a lower limiting value of N_{cc} below, which θ_{max} crosses its allowable limit.

Fig. 10 depicts the effect of A_r on the variation of θ_{max} with Q while the values of N_{cc} and Re_H are being kept constant at 0.40 and 2500, respectively. As expected, it can be noted that θ_{max} increases with increase in Q and for all values of A_r, this increase in θ_{max} with Q is almost linear. Further, it is important to note that there exists an upper limiting value of Q beyond which θ_{max} crosses its allowable limit.

In addition, it is worth noticing that as A_r increases from 5 to 10, other parameters being kept constant; there is a marginal increase in θ_{max} which is somewhat clearly visible for higher values of Q. Interestingly enough, it is quite important to note that further increase in A_r beyond 10 results in negligible increase in θ_{max}. The preceding observation of this figure is quite similar to that noticed in Fig. 8 and hence a similar conclusion can be drawn from this figure as well.

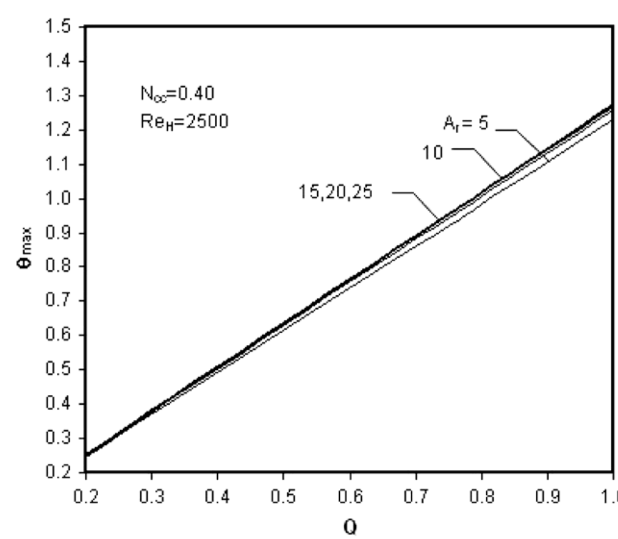

Fig. 10. The effect of A_r on the variation of θ_{max} with Q.

Fig. 11 depicts the effect of A_r on the variation of $\theta_{\max}$ with Re_H while the values of N_{cc} and Q are being kept constant at 0.40 and 0.75, respectively. As expected, it can be noticed that irrespective of the value of A_r, $\theta_{\max}$ decreases with increase in Re_H. Further, it is worth noticing that this rate of decrease in $\theta_{\max}$ is some what greater for lower values of Re_H as compared to its larger values. Furthermore, it is important to note that the effect of A_r on $\theta_{\max}$ vs. Re_H profiles is quite insignificant. Exactly similar observations were made while discussing the effect of A_r on $\theta_{\max}$ vs. N_{cc} and $\theta_{\max}$ vs. Q profiles depicted in Figs. 8 and 10, respectively.

Fig. 12 shows the effect of N_{cc} on the variation of $\theta_{\max}$ with Re_H while $A_r = 15$ and $Q = 0.75$ are being kept constant. As noticed from Fig. 11, it is more evident from this figure that irrespective of the values of N_{cc}, $\theta_{\max}$ decreases with increase in Re_H. Besides, it can be exclusively noted from this figure that the rate of this decrease in $\theta_{\max}$ for a lower value of N_{cc} is greater than that of higher value of N_{cc} and this is particularly true for lower values of Re_H. Further, it is also apparent from this figure that other parameters being kept constant, $\theta_{\max}$ decreases with increase in N_{cc} and the rate of this decrease diminishes with increase in N_{cc}. Furthermore, it is extremely important to note that other parameters being kept constant, there is a lower limiting value of Re_H below which $\theta_{\max}$ exceeds its allowable limit. For example, it can be noted from this figure that for $A_r = 15$, $Q = 0.75$, and $N_{cc} = 0.50$, the lower limiting value of Re_H is 1150. It is important to note from this figure that for any particular value of Re_H, there exists a lower limiting value of N_{cc} below which the value of $\theta_{\max}$ crosses its allowable limit. It is also quite important to note from this figure that in order to keep $\theta_{\max}$ well within its allowable limit, Re_H can be decreased by increasing N_{cc}. Thus, it can be concluded that keeping $\theta_{\max}$ well within its allowable limit, coolant pumping power requirement can be drastically reduced merely by increasing the value of N_{cc}.

Fig. 13 depicts the effect of Q on the variation of $\theta_{\max}$ with Re_H while keeping $A_r = 15.0$ and $N_{cc} = 0.40$ as constant. It can be seen that irrespective of the value of Q, $\theta_{\max}$ vs. Re_H profiles is similar to those illustrated in Figs. 11 and 12 for different values of A_r and N_{cc}, respectively. Besides, it can be noticed from this figure that the rate of decrease in $\theta_{\max}$ with respect to increase in Re_H diminishes as Q decreases, which is particularly true for lower values of Re_H. Further, it is quite obvious from this figure that irrespective of the value of Re_H, the increase in $\theta_{\max}$ is proportional to the increase in Q. Furthermore, it is quite important to note that for a set of constant value of A_r, N_{cc}, and Re_H, there is an upper limiting value of Q beyond which $\theta_{\max;}$ exceeds its allowable limit.

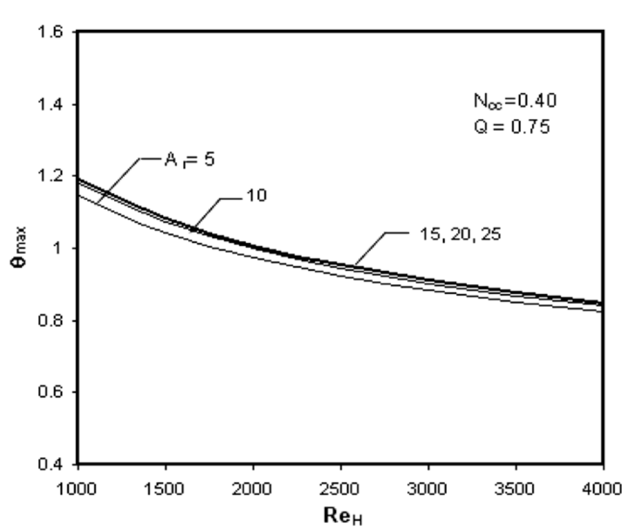

Fig. 11. The effect of A_r on the variation of $\theta_{\max}$ with Re_H.

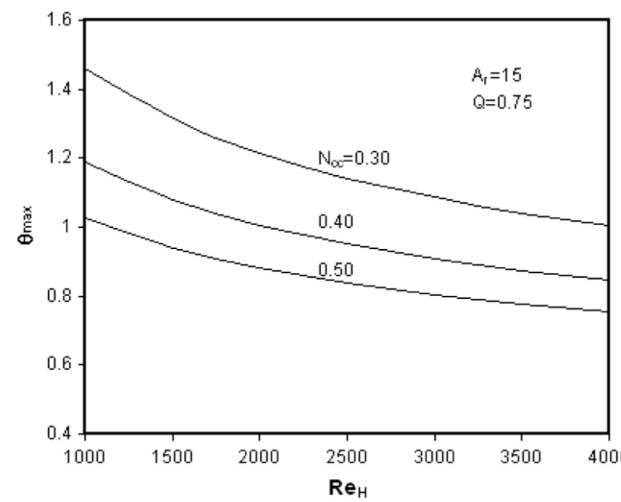

Fig. 12. The effect of N_{cc} on the variation of $\theta_{\max}$ with Re_H.

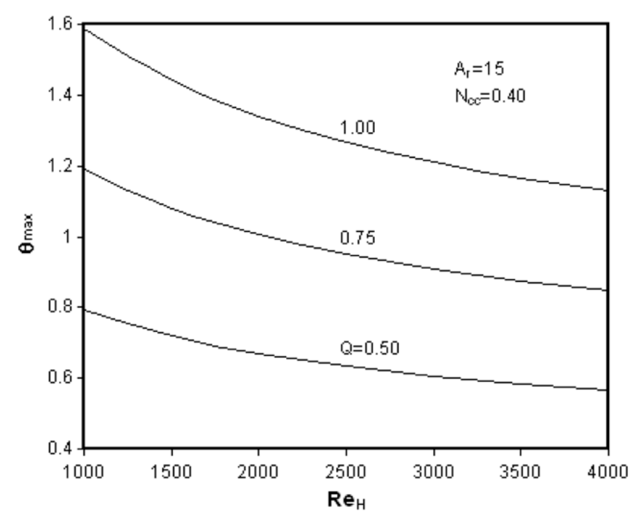

Fig. 13. The effect of Q on the variation of $\theta_{\max}$ with Re_H.

5. Conclusions

The present paper aims at fulfilling two objectives – the first, to establish the criterion for the boundary layer solution to be accurate enough in the study of conjugate heat transfer problem associated with a rectangular nuclear fuel element washed by upward moving coolant and the second, to present a critical analysis of the variation of $\theta_{\max}$ with A_r, N_{cc}, Q, and Re_H Accordingly, employing stream function–vorticity formulation and second-order accurate finite difference schemes, the Navier–Stokes and the energy equations governing the flow and thermal fields in the coolant are solved simultaneously with the equation governing the steady two-dimensional temperature distribution in the plate by satisfying the conditions of continuity of temperature and heat flux at the solid–fluid interface. Keeping the value of Pr for liquid sodium to be constant at 0.005, numerical results are presented and discussed in detail for a wide range of the involved parameters. From detailed discussion of these numerical results, following important conclusions are drawn:

- For all values of $A_r \geqslant 15$, the numerical predictions based on boundary layer approximations are accurate enough.

- For a given set of involved parameters, there is an upper limiting value of A_r beyond which increase in $\theta_{\max}$ is negligible.
- For a given thermal power capacity of the nuclear reactor, coolant pumping power requirement can be minimized merely by selecting a higher value of N_{cc}.

References

[1] S. Jahangeer, M.K. Ramis, G. Jilani, Conjugate heat transfer analysis of a heat generating vertical plate, Int. J. Heat Mass Transfer 50 (2007) 85–93.
[2] M.K. Ramis, G. Jilani, S. Jahangeer, Conjugate conduction–forced convection heat transfer analysis of a rectangular nuclear fuel element with non-uniform volumetric energy generation, Int. J. Heat Mass Transfer 51 (2008) 517–525.
[3] T.L. Perelman, On conjugated problems of heat transfer, Int. J. Heat Mass Transfer 3 (1961) 293–303.
[4] A.V. Luikov, Conjugate convective heat transfer problems, Int. J. Heat Mass Transfer 17 (1974) 257–265.
[5] P. Payvar, Convective heat transfer to laminar flow over a plate of finite thickness, Int. J. Heat Mass Transfer 20 (1977) 431–433.
[6] A. Pozzi, M. Lupo, The coupling of conduction with forced convection over a flat plate, Int. J. Heat Mass Transfer 32 (1989) 1207–1214.
[7] W.-S. Yu, H.-T. Lin, T.-Y. Hwang, Conjugate heat transfer of conduction and forced convection along wedges and a rotating cone, Int. J. Heat Mass Transfer 34 (1991) 2497–2507.
[8] I. Pop, D.B. Ingham, A note on conjugate forced convection boundary layer flow past a flat plate, Int. J. Heat Mass Transfer 36 (1993) 3873–3876.
[9] C. Treviño, G. Becerra, F. Mèndez, The classical problem of convective heat transfer in laminar flow over a thin finite thickness plate with uniform temperature at the lower surface, Int. J. Heat Mass Transfer 40 (1997) 3577–3580.
[10] K. Chida, Surface temperature of a flat plate of finite thickness under conjugate laminar forced convection heat transfer condition, Int. J. Heat Mass Transfer 43 (2000) 639–642.
[11] E.M. Sparrow, M.K. Chyu, Conjugate forced convection–conduction analysis of heat transfer in a plate fin, ASME J. Heat Transfer 104 (1982) 204–206.
[12] B. Sunden, The effect of Prandtl number on conjugate heat transfer from rectangular fins, Int. Comm. Heat Mass Transfer 12 (1985) 225–232.
[13] V.K. Garg, K. Velusamy, Heat transfer characteristics for a plate fin, ASME J. Heat Transfer 108 (1986) 224–226.
[14] M.J. Huang, C.K. Chen, Conjugate forced convection–conduction plate fin in power law fluids, Int. Comm. Heat Mass Transfer 14 (1987) 371–380.
[15] B. Sunden, Analysis of conjugated laminar and turbulent forced convection–conduction heat transfer of a plate fin, Int. Comm. Heat Mass Transfer 16 (1989) 821–831.
[16] M. Vynnycky, S. Kimura, K. Kanev, I. Pop, Forced convection heat transfer from a flat plate: the conjugate problem, Int. J. Heat Mass Transfer 41 (1998) 45–59.
[17] P.R. Kanna, M.K. Das, Conjugate forced convection heat transfer from a flat plate by laminar plane wall jet flow, Int. J. Heat Mass Transfer 43 (2005) 2896–2910.
[18] R. Karvinen, Some new results for conjugated heat transfer in a flat plate, Int. J. Heat Mass Transfer 21 (1978) 1261–1264.